Generalized polynomial chaos and stochastic collocation methods for uncertainty quantification in aerodynamics

Jacques Peter, Eric Savin, Itham Salah el Din
DAAA, DTIS
ONERA, Université Paris Saclay
29 avenue de la Division Leclerc
92322 Chtillon
FRANCE

Jacques.Peter@onera.fr

ABSTRACT

The maturity of CFD and the variability of operational and geometrical parameters in fluid dynamics analysis and design lead to the development of Uncertainty Quantification (UQ). Among the numerous methods for (UQ), these lecture notes describe the main features of Monte-Carlo and metamodel-based Monte-Carlo (§2), generalized Polynomial Chaos (§3) and Stochastic Collocation (§4). Also presented are Smolyak's sparse quadratures (§5) and Sobol' indices (§6). Three applications of (UQ) to (2D) and (3D) RANS flows, that have been carried out at ONERA, are finally described (§7).

Contents

1.0 INTRODUCTION

For many applications of Fluid Dynamics, either in flow analysis or shape optimization, operational or geometrical parameters of the problem may be subject to small variations. Cruise, for example, is known to be a flow condition of first importance for an aircraft and, in first approximation, the cruise Mach number is known to be constant. Actually, it happens that an aircraft slows down to arrive at exact time of landing slot, or that it speeds up to cope with the pilot maximum flight time. Mach number of cruise flight is hence subject to small variations that can be modeled by a probability density function and cruise drag evaluation should integrate drag times this density function over the domain of actual cruise Mach numbers.

The maturity of CFD and the variability of operational and geometrical parameters in fluid dynamics problems of analysis and design lead to the development of Uncertainty Quantification (UQ). Most often the CFD methods for (UQ) aim at (1) calculating mean and variance of outputs of interest; (2) predicting the range of an output under (a) stochastic parameter(s) variation; (3) predicting the probability that an output exceeds a threshold.

Among the numerous methods for (UQ), these lecture notes describe the main features of Monte-Carlo and (non-specific) metamodel-based-Monte-Carlo (§2) ; generalized Polynomial Chaos (§3) and Stochastic Collocation (§4). The broadly used sparse grid quadrature method of Smolyak [11] is then presented (§5). Two

applications of (UQ) to (2D) and (3D) RANS flows, that have been carried out at ONERA, are finally presented (§6).

2.0 PROBABILITY BASICS, MONTE-CARLO, SURROGATE-BASED MONTE-CARLO

2.1 Probability basics

The classical framework of probability spaces is a general mathematical structure that is suitable for both discrete and continuous stochastic variables. A probability space consists of:

- a sample space Ω (dice values, interval of Mach number values) that is the set of all outcomes
- a set of events space $\mathcal{A}$ (σ-algebra), consisting of elements of Ω or sets of elements of Ω, stable by union, intersection, including null set $\emptyset$ and Ω (pair of dice values, set of even dice values... subinterval of Mach number values...)
- The assignment of probabilities to the events of $\mathcal{A}$ satisfying the intuitive rules for union and intersection

In a probability problem, the inputs are precisely the sample space, set of events and probability function of the events. The outputs are random variable depending on the events. Typically, in UQ involving CFD, events are stochastic inputs of the flow simulation like stochastically varying free-stream Mach number or angle of attack whereas random variables are classical CFD outputs like CDp, CLp... or friction, pressure distribution at the walls... that depend on the stochastic inputs via the calculation of flow.

Discrete example : regular 6-face dice thrown once

- event ξ = 1,2,3,4,5 or 6
- sample space Ω ={1,2,3,4,5,6}
- set of events (σ-algebra) $\mathcal{F}$ = null set plus all discrete sets of these numbers $\{\emptyset, \{1\}, \{2\}, \{3\}, \{4\}, \{5\}, \{6\}, \{1,2\}, \{1,3\}, \{1,4\}, \{1,5\}, \{1,6\}, \{2,3\}, \{2,4\}, \{2,5\}$ ... $\{1,2,3,4,5,6\}\}$
- probability function P : $P(\emptyset) = 0$, $P(\{1\}) = 1./6.$, $P(\{2\}) = 1./6.$,... $P(\{1,2\}) = 1./3.$, $P(\{1,3\}) = 1./3$, $P(\{1,4\}) = 1./3$.... $P(\{1,2,3,4,5,6\}) = 1.$
- random variables X: dice value to the power three...

Continuous example : Far-field Mach number in [0.81,0.85]

- event ξ = a Mach number value in [0.81,0.85]
- sample space Ω = [0.81,0.85]
- set of events (σ-algebra) $\mathcal{F}$ = all subparts of [0.81,0.85]
- probability function P. Probability of an element I of $\mathcal{F}$ to be defined as the integral of probability density function, D, over I. For example:

$$D(\phi) = \frac{35}{32}(1. - \phi^2)^3 \quad \phi \in [-1, 1] \qquad\qquad \phi = (\xi - 0.83)/0.02$$

$$D_\xi(\xi) = \frac{1}{0.02} D(\phi) = \frac{1}{0.02}\frac{35}{32}(1. - (\frac{\xi - 0.83}{0.02})^2)^3$$

- possible random variables X = lift, drag, pitching moment of a wing... with variable Mach number M_∞ ("event" ξ) in the far-field

There are many classical probability density functions. For engineering purpose where, most often, stochastic variables have finite upper and lower bounds, the so called β-distribution is often well-suited. It has two exponent parameters denoted α and β that allow to vary the shape of the pdf from flat (α,β)=(1,1) to very peaky (high α and β). Distinct parameters lead to skewed distributions. The formula of these probability density functions on $[X_m, X_M]$ (with the $a-1$, $b-1$ convention for exponents) is

$$\beta_{\mathrm{I}}(x; a, b) = \mathbb{1}_{[X_m, X_M]}(x) \frac{\Gamma(a+b)}{\Gamma(a)\Gamma(b)} \frac{(x - X_m)^{a-1}(X_M - x)^{b-1}}{(X_M - X_m)^{a+b-1}}. \tag{1}$$

2.2 Monte-Carlo

Monte-Carlo mimics the law of the events in a series of calculations. It is the reference method for all uncertainty propagation methods. A presentation of the method is given hereafter for one uncertain parameter and a scalar random variable.
Classical stochastic toolboxes provide sampling $(\xi^1, \xi^2 ..., \xi^p ..., \xi^N ...)$ for any standard p.d.f $D(\xi)$. The corresponding flow fields, $W(\xi^p), p \in [1, N]$, depending on the stochastic parameter ξ (variable angle of attack...) have to be computed. The corresponding functional outputs $\mathcal{J}(\xi^p) = J(W(\xi^p))$ have then to be calculated. The classical unbiased Monte-Carlo estimations of mean and variance are the following:

$$E(\mathcal{J}) = \int \mathcal{J}(\xi) D(\xi) d\xi \simeq \bar{\mathcal{J}}_N = \frac{1}{N} \sum_{p=1}^{p=N} \mathcal{J}(\xi^p),$$

$$\sigma^2_{\mathcal{J}} = E((\mathcal{J} - E(\mathcal{J}))^2) = \int (\mathcal{J}(\xi) - E(\mathcal{J}))^2 D(\xi) d\xi \simeq \sigma^2_{\mathcal{J}_N} = \frac{1}{N-1} \sum_{p=1}^{p=N} (\mathcal{J}(\xi^p) - \bar{\mathcal{J}}_N)^2.$$

What is the accuracy of these estimates ?

2.2.1 Accuracy of estimated mean, known variance

When variance $\sigma_{\mathcal{J}}$ is known, the convergence in law of the mean [1] is characterized by

$$\sqrt{N} \frac{\bar{\mathcal{J}}_N - E(\mathcal{J})}{\sigma_{\mathcal{J}}} \rightsquigarrow \mathcal{N}(0, 1) \tag{2}$$

where $\mathcal{N}(0, 1)$ is the Normal distribution which probability density function $D_{\mathcal{N}}(x)$ and symmetric cumulative distribution $\Phi_{\mathcal{N}}(x)$ are

$$D_{\mathcal{N}}(x) = \frac{1}{\sqrt{2\Pi}} e^{-\frac{x^2}{2}} \qquad \Phi_{\mathcal{N}}(x) = \frac{1}{\sqrt{2\Pi}} \int_{-x}^{x} e^{-\frac{t^2}{2}} dt.$$

[1] Note that the mean of a well defined stochastic variable does not always exist. Consider $pdf(x) = \frac{2}{\Pi} \frac{1}{1+x^2}$ for $x > 0$

Equation (2) translates in propositions like (with a symmetric interval):

$$\textit{With } \epsilon \textit{ confidence } \quad E(\mathcal{J}) \in [\bar{\mathcal{J}}_N - u_\epsilon \frac{\sigma_\mathcal{J}}{\sqrt{N}}, \bar{\mathcal{J}}_N + u_\epsilon \frac{\sigma_\mathcal{J}}{\sqrt{N}}] \quad \textit{where } \epsilon = \frac{1}{\sqrt{2\Pi}} \int_{-u_\epsilon}^{u_\epsilon} e^{-\frac{t^2}{2}} dt.$$

Table 1 provides some numerical values of u_ϵ and, for example

$$\textit{With } 99\% \textit{ confidence } \quad E(\mathcal{J}) \in [\bar{\mathcal{J}}_N - 2.576 \frac{\sigma_\mathcal{J}}{\sqrt{N}}, \bar{\mathcal{J}}_N + 2.576 \frac{\sigma_\mathcal{J}}{\sqrt{N}}] \quad \textit{as } \quad 0.99 = \frac{1}{\sqrt{2\Pi}} \int_{-2.576}^{2.576} e^{-\frac{t^2}{2}} dt.$$

2.2.2 Accuracy of estimated mean, unknown variance

In the common practical case where the variance $\sigma_\mathcal{J}$ is not known, the law for mean convergence is

$$\sqrt{N} \frac{\bar{\mathcal{J}}_N - E(\mathcal{J})}{\sigma_{\mathcal{J}_N}} \rightsquigarrow \mathcal{S}(N-1) \tag{3}$$

where $\mathcal{S}$ is the Student distribution. Equation (3) translates in proposition like :

$$\textit{With } \epsilon \text{ confidence } \quad E(\mathcal{J}) \in [\bar{\mathcal{J}}_N - u_{\epsilon_{(N-1)}} \frac{\sigma_{\mathcal{J}_N}}{\sqrt{N}}, \bar{\mathcal{J}}_N + u_{\epsilon_{(N-1)}} \frac{\sigma_{\mathcal{J}_N}}{\sqrt{N}}]$$

where $u_{\epsilon_{N-1}}$ as function of ϵ and N can be found in tables. Student distribution converges to Normal distribution for large N and u_{ϵ_N} decreases when N increases. Some numerical values of $u_{\epsilon_{N-1}}$ are given in Table 2. The probability density function of Student distribution is

$$D_{\mathcal{S}(N)}(x) = \frac{\Gamma(\frac{N+1}{2})}{\Gamma(\frac{N}{2})\sqrt{N\Pi}} (1 + \frac{x^2}{N})^{-\frac{N+1}{2}} \qquad \left(\Gamma(u) = \int_0^{+\infty} t^{u-1} e^{-t} dt \right)$$

and, of course, a more precise convergence property may then be presented

$$\textit{With } \epsilon \textit{ confidence } \quad E(\mathcal{J}) \in [\bar{\mathcal{J}}_N - u_{\epsilon_{(N-1)}} \frac{\sigma_{\mathcal{J}_N}}{\sqrt{N}}, \bar{\mathcal{J}}_N + u_{\epsilon_{(N-1)}} \frac{\sigma_{\mathcal{J}_N}}{\sqrt{N}}] \quad \textit{where } \epsilon = \int_{-u_{\epsilon_{N-1}}}^{u_{\epsilon_{N-1}}} D_{\mathcal{S}(N-1)}(t) dt$$

ϵ	0.5	0.9	0.95	0.99
u_ϵ	0.674	1.645	1.960	2.576

Table 1: Value of u_ϵ for normal distribution

ϵ N	2	3	20	30	∞
0.95	12.71	4.303	2.093	2.045	1.960
0.99	63.66	9.925	2.861	2.756	2.576

Table 2: Value of $u_{\epsilon(N-1)}$ for Student distribution $\mathcal{S}(N-1) \quad N \geq 2$

2.2.3 Accuracy of estimated variance

Accuracy of estimated variance $\mathcal{J}_N$ is discussed in the slides provided to the attendance in both cases of known and unknown mean.

2.2.4 Convergence speed of Monte-Carlo method

A typical realistic estimation of accuracy of mean estimated by Monte-Carlo is: For a N-point sampling, with 99% confidence,

$$E(\mathcal{J}) \in [\bar{\mathcal{J}}_N - u_{0.99,(N-1)}\frac{\sigma_{\mathcal{J}_N}}{\sqrt{N}}, \bar{\mathcal{J}}_N + u_{0.99,(N-1)}\frac{\sigma_{\mathcal{J}_N}}{\sqrt{N}}],$$

with $u_{0.99,1} = 63.66$, $u_{0.99,2} = 9.925$, $u_{0.99,3} = 5.841$, $u_{0.99,9} = 3.250$, $u_{0.99,19} = 2.861$, $u_{0.99,19} = 2.756$,... decreasing with the number of samples, N, towards the limiting value, 2.576. The convergence speed of Monte-Carlo for mean value estimation is hence $\frac{1}{\sqrt{N}}$ and increasing the precision of Monte-Carlo estimation by a factor of 10 requires multiplying the number of evaluations by a factor of 100. This is a very slow convergence and a very expensive method if one evaluation requires the numerical solution of Euler or (RANS) equations.

Besides the outputs of many types of CFD calculations are very regular functions of the parameters of interest and it is necessary to take advantage of this property. In metamodeling approaches, precisely, the regularity of the random variables (then first seen as output variables) as function of stochastic variables (then first seen as regular input variables) is exploited. There are many types of surrogates can be combined with Monte-Carlo (discussed next subsection 2.3). Besides there are specific polynomial expansions associated to the probability density function (discussed in sections 3 and 4). The common feature of all this surrogate-based methods is that all stochastic quantities of interest – mean, variance, kurtosis, range, risk... – are estimated for the surrogate instead of the exact function of interest.

2.3 Surrogate-based Monte-Carlo

Metamodel-based Monte-Carlo first requires the definition of a surrogate of the output(s) of interest on the space of stochastic parameters. This is typically done with the metamodeling toolboxes that are mainly used for global optimization and include steps of inner parameter calculation and design of experiment enrichment. Basically all types of surrogates may be used: Kriging, Radial Basis Function, Support Vector Regression, adjoint based quadratic Taylor expansion... After this non-stochastic step has been carried out, stochastic evaluations are performed based on the (cheap) approximate output values provided by the surrogate. Figure 1 is a scheme of this process[2]. The asset of surrogate-based Monte-Carlo is illustrated with a simple and demonstrative example: The flow about a NACA0012 profile is considered at following flow conditions

$$M = 0.73, Re = 6.10^6, AoA = 3^\circ.$$

The angle of attack is assumed to have stochastic variations and the stochastic behavior of the lift, C_L, is to be studied. The pdf of the angle of attack – varying in $[2.9^o, 3.1^o]$ – is a beta-distribution:

$$D_a(\alpha) = 10D_b(10.(\alpha - 3.)) \qquad D_b(\xi) = \frac{15}{16}(1-\xi)^2(1+\xi)^2.$$

(RANS)&(k-w) calculations is run with the elsA code [1] using standard numerical discretizations for a series of 11 Tchebychev points in the interval of angle of attack. For the corresponding 11 values of the lift, C_L, very

[2]The authors are not aware of any publication discussing the influence of the metamodel accuracy on accuracy of stochastic quantities (mean, variance...)

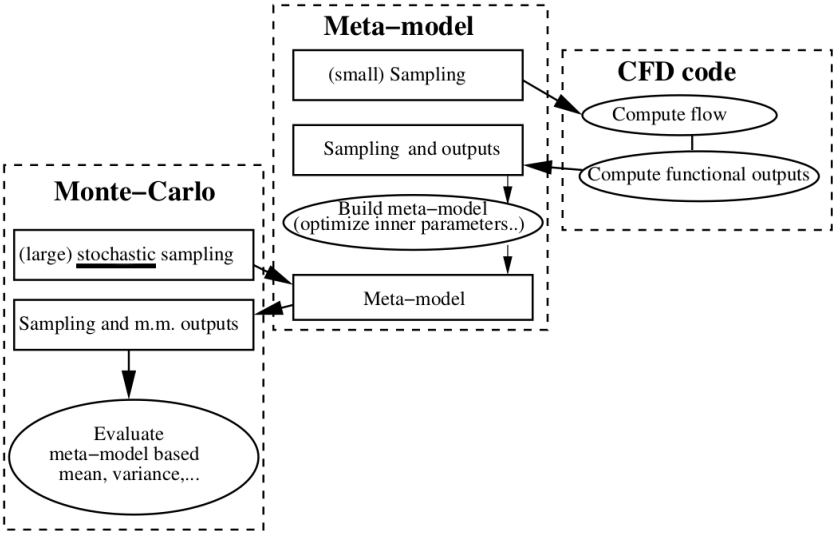

Figure 1: Monte-Carlo method with meta-models

regular identical curves are built by Ordinary Kriging, Radial Basis Function and Support Vector Regression – see figure 2. These almost linear curves, obtained with three different metamodels, for a quantity that is often assumed to be linear as function of low angles of attacks, suggest a very accurate surrogate representation of the lift on the parameter domain that can be used instead of CFD calculations for stochastic evaluations. This has been done and is illustrated by figures 3 and 4. With CFD-based Monte-Carlo, with the fixed budget, only 100 CFD evaluations could be run. This yields the 90, 95 and 99 confidence intervals for lift and variance that appear in the left part of figure 3 and 4 for the considered stochastic sampling. When using metamodel-based Monte-Carlo, up to one million sampling points can be used reducing the intervals of confidence to smaller intervals than generally needed – right part of figures 3 and 4.

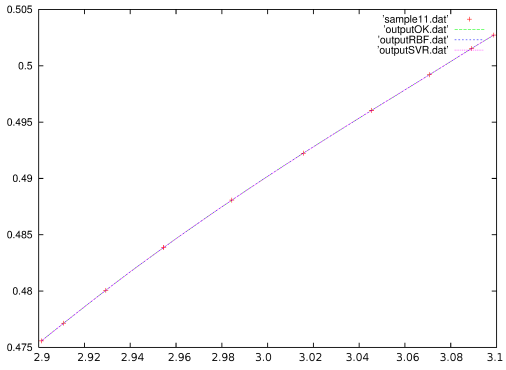

Figure 2: NACA0012 C_L, as function of the Angle of Attack

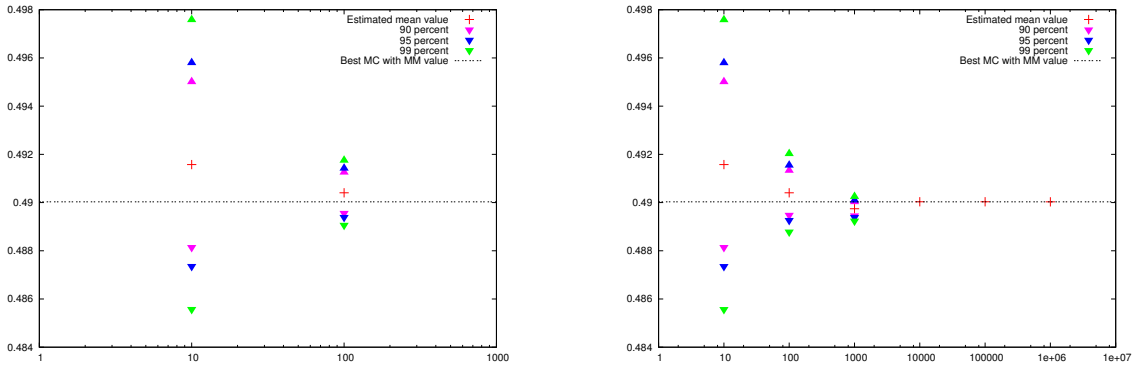

Figure 3: Mean of C_L coefficient and confidence interval (left CFD evaluations, right metamodel)

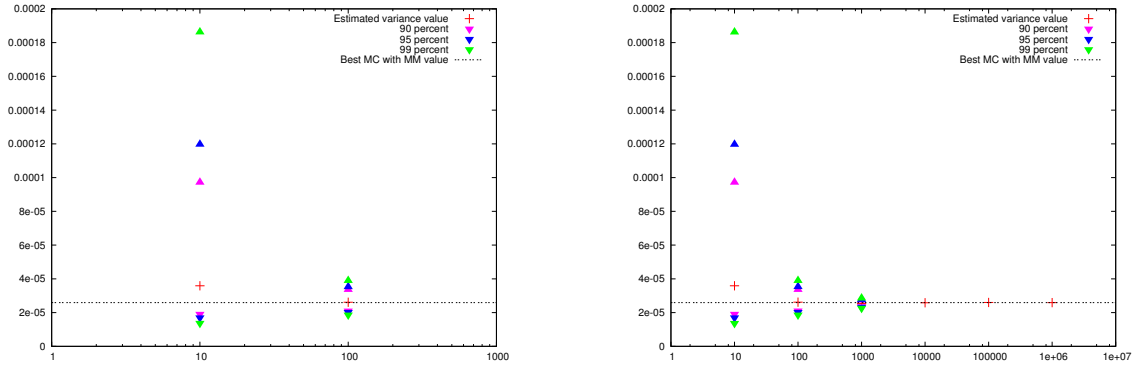

Figure 4: Mean of C_L coefficient and confidence interval (left CFD evaluations, right metamodel)

3.0 GENERALIZED POLYNOMIAL CHAOS

Generalized Polynomial Chaos (gPC) is a spectral expansion method [5, 13, 14]. For a single real output F and a single real stochastic input, ξ, this expansion (denoted gF) reads

$$gF(\xi) = \sum_{l=0}^{l=M} C_l P_l(\xi) \simeq F(\xi), \tag{4}$$

where P_l is a polynomial of degree l and where the $\{P_l\}_{l\in\{1...M\}}$ form an orthonormal basis for the dot product defined by the p.d.f. $D(\xi)$:

$$< P_l, P_m >= \int P_l(\xi) P_m(\xi) D(\xi) d\xi = \delta_{lm}. \tag{5}$$

The main asset of the method is the straightforward calculation of the mean and variance of (gPC) expansions. More generally, all possible stochastic post-processing for F is done for the specific surrogate gF (which difference w.r.t. exact function F may be discussed in the framework of spectral expansion theory).
The method is presented in 1D (one uncertain parameter) and then in 2D (two uncertain parameters), the generalization from 2D to dD being straightforward.

3.1 Families of orthonormal polynomials

The classical probability density functions are associated to a family of polynomials that is orthogonal w.r.t. it in the sense of equation (5). The correspondence between classical p.d.f. and classical families of polynomials is the following:

- Normal distribution $D_n(\xi) = \frac{1}{\sqrt{2\Pi}} e^{-\frac{\xi^2}{2}}$ on $\mathbb{R}$ $\rightarrow$ Hermitte polynomials
- Gamma distribution $D_g(\xi) = exp(-\xi)$ on $\mathbb{R}^+$ $\rightarrow$ Laguerre polynomials
- Uniform distribution $D_u(\xi) = 0.5$ on $[-1, 1] \rightarrow$ Legendre polynomials
- Chebyshev distribution $D_{cf}(\xi) = 1/\Pi/\sqrt{1-\xi^2}$ on $[-1, 1] \rightarrow$ Chebyshev (first-kind) polynomials
- Chebyshev distribution $D_{cs}(\xi) = \sqrt{1-\xi^2}$ on $[-1, 1] \rightarrow$ Chebyshev (second-kind) polynomials
- Beta-distribution $D_\beta(\xi) = (1-\xi)^\alpha (1+\xi)^\beta / \int_{-1}^{1} (1-u)^\alpha (1+u)^\beta du \quad \alpha > -1. \ , \beta > -1.$ on $[-1, +1]$ $\rightarrow$ Jacobi polynomials (including Chebyshev polynomials)
- Non-usual probabilistic density functions, $D_l(\xi)$, polynomials computed by Gram-Schmidt orthogonalisation process.

Most often, the families of polynomials that satisfy the classical 3-term recurrence relation and exhibit the associated properties are orthogonal but not orthonormal for the functional dot product (5). This is illustrated with Hermitte polynomials associated to normal law $D_n(\xi) = \frac{1}{\sqrt{2\Pi}} e^{-\frac{\xi^2}{2}}$. The first polynomials are

$$\overline{PH}_0(\xi) = 1 \qquad \overline{PH}_1(\xi) = \xi \qquad \overline{PH}_2(\xi) = \xi^2 - 1 \qquad \overline{PH}_3(\xi) = \xi^3 - 3\xi$$

The recursive definition is based on $\overline{PH}_0(\xi)$, $\overline{PH}_1(\xi)$ and $\overline{PH}_{n+1}(\xi) = \xi \overline{PH}_n(\xi) - n\overline{PH}_{n-1}(\xi)$ A normalization of the standard Hermitte polynomial is required

$$PH_j(\xi) = \frac{1}{\sqrt{j!}} \overline{PH}_j(\xi),$$

to define a family of proportional polynomials $\{PH\}$ that is orthonormal for D_n

$$\left(\text{ meaning that } \quad < PH_j, PH_k >= \int_{-\infty}^{+\infty} PH_j(\xi) PH_k(\xi) D_n(\xi) d\xi = \delta_{jk} \right)$$

and hence suitable for (gPC) method.

3.2 Calculation of coefficients by quadrature

The (gPC) coefficients C_l can be calculated by quadrature or by collocation. Concerning the first method, let us first note that $C_l =< gF, P_l >$ that is immediately proved multiplying equation (4) by $P_l(\xi)D(\xi)$ and integrating over the domain of variation of ξ. Actually, under regularity assumptions, $C_l =< F, P_l >$ and coefficient calculation by quadrature relies on this expression.
Any classical 1D quadrature can be used to compute the

$$C_l =< F, P_l >= \int F(\xi) P_l(\xi) D(\xi) d\xi \quad l \in \{0...M\} \tag{6}$$

coefficients. Due to the presence of the term $D(\xi)$ in equation (6), the g-point Gaussian quadrature associated to D is a natural choice. The formula of this quadrature is

$$\int h(\xi)D(\xi)d\xi \simeq \sum_{k=1}^{k=g} w_k h(\xi_k)$$

(where obviously (w_k,ξ_k) depend on $D(\xi)$). This formual is exact if h is a polynomial of degree up to degree $(2g-1)$. What would be a satisfactory number of points to calculate the coefficients ? A reasonable heuristic choice requires that polynomials P_l be orthonormal at the discrete level. As the maximum degree of the product of two polynomials of the basis is $2M$, twice the expansion degree, the number of quadrature points should verify

$$2M \leq 2g-1,$$

to fulfill the discrete orthonormality requirement.

3.3 Calculation of coefficients by collocation

Basically, collocations consists in forcing equality of F and gF for $M+1$ values of ξ. The corresponding linear system reads

$$\sum_{l=0}^{l=M} C_l P_l(\xi_k) = F(\xi_k) \quad \forall\, k \in \{1, M+1\} \qquad \text{to solve for} \quad C_l.$$

In this simple case where the sample cardinal is the number of unknowns, (M+1), a linear system for the coefficients is solved. If the number of sampling evaluations $F(\xi_l)$ is larger than the number of unknown coefficients, (M+1), a least square problem has to be solved.
Finally, anticipating a very short presentation of the application of a method called “compressed sensing”, in section (§6.2) the collocation equations are rewritten in matrix form : $\mathbf{F}$ being the column vector of F values, $\mathbf{C}$ being the column vector of unknown polynomial coefficients and $\mathbf{K}$ being the matrix with terms $K_{ij} = P_j(\xi_i)$, the collocation set of linear equations reads

$$\mathbf{KC} = \mathbf{F}.$$

3.4 Stochastic post-processing

Stochastic post-processing is done for gF, the gPC approximation of F. The mean calculation reads

$$E(gF(\xi)) = \int \left(\sum_{l=0}^{l=M} C_l P_l(\xi) \right) D(\xi)d\xi = C_0,$$

due to orthonormality of the $P_l \;\; l \geq 1$ to P_0 or any other scalar factor (in other terms, the integral of the $P_l \;\; l > 1$ is zero). The mean value of $gF(\xi)$ with $D(\xi)$ as stochastic distribution of the input ξ is hence the first coefficient of the expansion. The calculation of gF variance is also very simple thanks to orthonormality of the polynomial basis :

$$E((gF(\xi) - C_0)^2) = \int \left(\sum_{l=1}^{l=M} C_l P_l(\xi) \right)^2 D(\xi)d\xi = \sum_{l=1}^{l=M} C_l^2.$$

The variance is the sum of the square of all coefficients but C_0.

As in surrogate-based Monte-Carlo, any other stochastic quantity is estimated for gF, the gPC surrogate. The skewness, for example is calculated as

$$E\left(\left(\frac{gF(\xi)-\mu}{\sigma}\right)^3\right) = \frac{1}{(\sum_{l=1}^{l=M} C_l^2)^{3/2}} \int \left(\sum_{l=1}^{l=M} C_l P_l(\xi)\right)^3 D(\xi)d\xi,$$

that requires the knowledge or the calculation of the $\int P_l(\xi)P_n(\xi)P_p(\xi)D(\xi)d\xi$ integrals. The range of F would be estimated sampling for ξ and searching for the range of $gF(\xi)$. Just as the same, the probability that F exceeds a threshold T would be approximated as

$$\int 1_{\{gF(\xi)>T\}} D(\xi)d\xi$$

and derived from a sampling of gF.

3.5 Case of vector outputs

Generalized polynomial chaos can be applied to scalar outputs as presented in previous sections but also to vector fields. Line or surface wall distribution of pressure or other aerodynamic variables are typical vector fields to which the gPC method would be applied. The extension of previous equations is rather simple. For a general presentation, a generic mesh index, i, and the stochastic variable ξ are the arguments of a field $W(i,\xi)$. The corresponding gPC expansion reads

$$gW(i,\xi) = \sum_{l=0}^{l=M} C_l(i)P_l(\xi) \qquad gW(i,\xi) \simeq W(i,\xi).$$

For a fixed mesh index i, all formulas of previous sections can be applied. In particular, the estimation of mean and variance are

$$E(gW(i,\xi)) = \int \left(\sum_{l=0}^{l=M} C_l(i)P_l(\xi)\right) D(\xi)d\xi = C_0(i),$$

$$E((gW(i,\xi)-C_0(i))^2) = \int \left(\sum_{l=1}^{l=M} C_l(i)P_l(\xi)\right)^2 D(\xi)d\xi = \sum_{l=1}^{l=M} C_l(i)^2.$$

3.6 Extension to d-D

Before discussing sparsification of output polynomial expansions and sparsification of quadratures in section §5, a full-tensorial extension of the 1D gPC method is considered. The presentation is done in 2D but the extension to dD is then straightforward.
The joint probability of the 2 uncertain parameters $(\xi_1,\xi_2) \in \mathrm{I}^1 \times \mathrm{I}^2$ is assumed to have the simple form

$$D(\xi_1,\xi_2) = D^\alpha(\xi_1)D^\beta(\xi_2).$$

The orthogonal polynomials associated to the dot products involving $D^\alpha(\xi_1)$ and $D^\beta(\xi_2)$ are respectively $(P_0^\alpha, P_1^\alpha, P_2^\alpha, ...)$ and $(P_0^\beta, P_1^\beta, P_2^\beta, ...)$. The 2D tensorial gPC expansion with $(M^1{+}1)$-point in direction 1, and $(M^2{+}1)$-point in direction 2, then reads

$$F(\xi_1,\xi_2) \simeq gF(\xi_1,\xi_2) = \sum_{k\le M^1, l\le M^2} C_{k,l} P_k^\alpha(\xi_1) P_l^\beta(\xi_2) \tag{7}$$

The description of the full-tensorial approach (that will highlight the interest of sparse approaches) then requires the definition of the tensorial product of two 1D quadratures. The tensor product of quadratures

$$A[f] = \sum_{k=1}^{k=g^\alpha} \omega_k^\alpha f(\xi_k^\alpha) \qquad \left(\text{approximating } \int_{\mathrm{I}^1} f(u)D^\alpha(u)du\right)$$

and

$$B[g] = \sum_{l=1}^{l=g^\beta} \omega_l^\beta g(\xi_l^\beta) \qquad \left(\text{approximating } \int_{\mathrm{I}^2} g(v)D^\beta(v)dv\right),$$

for integration over $\mathrm{I}^1 \times \mathrm{I}^2$ is denoted $(A \otimes B)$ and defined as

$$(A \otimes B)[h] = \sum_{k \leq g^\alpha, l \leq g^\beta} \omega_k^\alpha \omega_l^\beta h(\xi_k^\alpha, \xi_l^\beta).$$

The evaluation of a gPC coefficient by this quadrature reads

$$C_{k,l} = \int_{\mathrm{I}^1 \times \mathrm{I}^2} F(\xi_1, \xi_2) D^\alpha(\xi^1) D^\beta(\xi^2) d\xi_1 d\xi_2 \simeq (A \otimes B)[F] = \sum_{k \leq g^\alpha, l \leq g^\beta} \omega_k^\alpha \omega_l^\beta F(\xi_k^\alpha, \xi_l^\beta).$$

It requires $g^\alpha \times g^\beta$ flow calculations and evaluations of F. The coefficients of 2D expansion (7) could as well be calculated by collocation, identifying the spectral expansion for $(M^1+1) \times (M^2+1)$ points with exact evaluations

$$\sum_{k \leq M^1, l \leq M^2} C_{k,l} P_k^\alpha(\xi_1^s) P_l^\beta(\xi_2^s) = F(\xi_1^s, \xi_2^s) \qquad s \in \{1, 2, 3..., (M^1+1) \times (M^2+1)\}$$

As in the 1D case, the calculation of mean and variance of the expansion gF is simple thanks to the orthonormality of the basis

$$\begin{aligned}
E(gF) &= \int \left(\sum_{k \leq M^1, l \leq M^2} C_{k,l} P_k^\alpha(\xi_1) P_l^\beta(\xi_2) \right) d\xi_1 d\xi_2 = C_{0,0} \\
V(gF) &= E((gF - C_{0,0})^2) \\
&= \int \left(\sum_{k \leq M^1, l \leq M^2} C_{k,l} P_k^\alpha(\xi_1) P_l^\beta(\xi_2) D(\xi_1, \xi_2) d\xi_1 d\xi_2 - C_{0,0} \right)^2 D(\xi_1)^\alpha D^\beta(\xi_2) d\xi_1 d\xi_2 \\
&= \int \left(\sum_{k \leq M^1, l \leq M^2 \ (k,l) \neq (0,0)} C_{k,l} P_k^\alpha(\xi_1) P_l^\beta(\xi_2) \right)^2 D(\xi_1)^\alpha D(\xi_2)^\beta d\xi_1 d\xi_2 \\
&= \sum_{k \leq M^1, l \leq M^2 \ (k,l) \neq (0,0)} C_{k,l}^2
\end{aligned}$$

4.0 STOCHASTIC COLLOCATION

4.1 Expansion

Stochastic Collocation (SC) is another non-intrusive polynomial method [7]. It is based on Lagrangian polynomial expansion. It is first described for a vector field (generic mesh index i) in the 1D case (one uncertain parameter ξ). Given a set of $(M+1)$ distinct values of ξ (ξ_1, ξ_2... ξ_{M+1}), Stochastic Collocation is a dedicated polynomial expansion using Lagrangian polynomials

$$W(i,\xi) \simeq scW(i,\xi) = \sum_{l=1}^{l=M+1} W_l(i) H_l(\xi) \qquad H_l(\xi) = \prod_{m=1, m\neq l}^{m=M+1} \frac{(\xi - \xi_m)}{(\xi_l - \xi_m)}$$

where scW is a polynomial of degree M (sum of polynomials of degree M). We have to immediately note that

$$scW(i,\xi_l) = \sum_{l=1}^{l=N} W_l(i) H_l(\xi_l) = W_l(i).$$

There is hence no coefficient calculation step but the flow has to be computed for all $\xi_l \;\; l \in \{1...M+1\}$ and $W(i,\xi_l)$ has then to be derived from the whole field of state variables. Then, obviously

$$scW(i,\xi) = \sum_{l=1}^{l=M+1} W(i,\xi_l) H_l(\xi).$$

4.2 Stochastic post-processing

Although this is not absolutely mandatory (see the slides for two other cases), we consider here that (ξ_1, ξ_2... ξ_{M+1}) are the $M+1$ points of the $(M+1)$-point Gaussian quadrature associated to $D(\xi)$, the corresponding weights being $(\omega_1, \omega_2, ..., \omega_{M+1})$. As for generalized polynomial chaos method, the stochastic post-processing is done for scW instead of W.
The evaluation of mean value precisely uses the Gaussian quadrature which nodes are the same as those of the Lagrange set:

$$E(scW(i)) = \int scW(i,\xi) D(\xi) d\xi = \sum_{m=1}^{m=M+1} \omega_m scW(i,\xi_m) = \sum_{m=1}^{m=M+1} \omega_m W(i,\xi_m).$$

This calculation is exact as sCW is of degree M whereas the quadrature is exact for polynomials up to degree $(2M+1)$. Just as the same, the evaluation of variance is also based on the Gaussian quadrature and also exact (degree $2M$ polynomial)

$$\begin{aligned}
E((scW(i) - E(scW(i)))^2) &= E(scW(i)^2) - E(scW(i))^2 \\
&= \int scW(i,\xi)^2 D(\xi) d\xi - E(scW(i))^2 \\
&= \sum_{m=1}^{m=M+1} \omega_m scW(i,\xi_m)^2 - E(scW(i))^2 \\
&= \sum_{m=1}^{m=M+1} \omega_m W(i,\xi_m)^2 - \left(\sum_{m=1}^{m=M+1} \omega_m W(i,\xi_m) \right)^2
\end{aligned}$$

4.3 Extension to d-D

The presentation is done for 2 uncertain parameters $(\xi_1, \xi_2) \in \mathrm{I}^1 \times \mathrm{I}^2$, the extension to d-D being straightforward The joint probability distribution is assumed to be

$$D(\xi_1, \xi_2) = D^\alpha(\xi_1) D^\beta(\xi_2).$$

For the sake of simplicity, the method is presented for a scalar output. A tensorial grid of (M^1+1) and (M^2+1) Gauss-points associated to D^α and D^β is considered :

$$(\xi_1^\alpha, \xi_2^\alpha, ..., \xi_{M^1+1}^\alpha) \quad \times \quad (\xi_1^\beta, \xi_2^\beta, ..., \xi_{M^2+1}^\beta),$$

the weights being

$$(\omega_1^\alpha, \omega_2^\alpha, ..., \omega_{M^1+1}^\alpha) \qquad (\omega_1^\beta, \omega_2^\beta, ..., \omega_{M^2+1}^\beta).$$

The Lagrange polynomials associated to the two sets are

$$H_k^\alpha(\xi_1) = \prod_{m=1, m\neq k}^{m=M^1+1} \frac{(\xi_1 - \xi_m^\alpha)}{(\xi_k^\alpha - \xi_m^\alpha)} \qquad H_l^\beta(\xi_2) = \prod_{m=1, m\neq l}^{m=M^2+1} \frac{(\xi_2 - \xi_m^\beta)}{(\xi_l^\beta - \xi_m^\beta)}.$$

The stochastic collocation 2D expansion is

$$scF(\xi_1, \xi_2) = \sum_{k \leq M^1; l \leq M^2} d_{k,l} H_k^\alpha(\xi_1) H_l^\alpha(\xi_2) \qquad scF(\xi_1, \xi_2) \simeq F(\xi_1, \xi_2).$$

As in the 1D case, the coefficients of the expansion are easily identified as $d_{k,l} = F(\xi_k^\alpha, \xi_l^\beta)$, so that

$$scF(\xi_1, \xi_2) = \sum_{k \leq M^1; l \leq M^2} F(\xi_k^\alpha, \xi_l^\beta) H_k^\alpha(\xi_1) H_l^\beta(\xi_2).$$

The tensor product of the two Gaussian rules is defined as

$$\int F(\xi_1, \xi_2) D^\alpha(\xi_1) D^\beta(\xi_2) d\xi_1 d\xi_2 = \sum_{k \leq M^1+1; l \leq M^2+1} \omega_k^\alpha \omega_l^\beta F(\xi_k^\alpha, \xi_l^\beta).$$

It exactly integrates all monomials $\xi_1^p \xi_2^q$ such that $p \leq 2M^1 + 1$ and $q \leq 2M^2 + 1$. The calculation of the mean of scF reads

$$\int scF(\xi_1, \xi_2) D^\alpha(\xi_1) D^\beta(\xi_2) d\xi_1 d\xi_2 = \sum_{k \leq M^1+1; l \leq M^2+1} \omega_k^\alpha \omega_l^\beta scF(\xi_k^\alpha, \xi_l^\beta),$$

but, as $scF(\xi_k^\alpha, \xi_l^\beta) = F(\xi_k^\alpha, \xi_l^\beta)$,

$$E(scF) = \int scF(\xi_1, \xi_2) D^\alpha(\xi_1) D^\beta(\xi_2) d\xi_1 d\xi_2 = \sum_{k \leq M^1+1; l \leq M^2+1} \omega_k^\alpha \omega_l^\beta F(\xi_k^\alpha, \xi_l^\beta).$$

It is exact thanks to the property of polynomial exactness of the tensor Gaussian quadrature.
The calculation of the variance scF is also exact due to the degree of the involved polynomials:

$$\begin{aligned} V(scF) &= E((scF - E(scF))^2) = E(scF^2) - E(scF)^2 \\ &= \int scF(\xi_1,\xi_2)^2 D^\alpha(\xi_1) D^\beta(\xi_2) d\xi_1 d\xi_2 - E(scF)^2 \\ &= \sum_{k\leq M^1+1; l\leq M^2+1} \omega_k^\alpha \omega_l^\beta F(\xi_k^\alpha,\xi_l^\beta)^2 - \left(\sum_{k\leq M^1+1; l\leq M^2+1} \omega_k^\alpha \omega_l^\beta F(\xi_k^\alpha,\xi_l^\beta) \right)^2 \end{aligned}$$

4.4 Cost of tensorial methods

If we assume that the tensor (gPC) or (SC) method is applied in d-dimension with M point per direction then the number of required CFD calculations is M^d that is not sustainable if d is high. For example, with 9 points per direction, the required number of simulations is

$$9^2 = 81 \quad 9^4 = 6561 \quad 9^5 = 59049 \quad 9^6 = 531441 \quad 9^8 = 43.046721 \quad 9^{10} = 3.486.784401$$

that is only feasible at reasonable cost up to d = 4 or 5. This increasing cost with the number of dimension is called *Curse of dimensionality*.

This is the reason why polynomials in total degree t are considered. They involve

$$Z = \binom{d+t}{d}$$

terms. It is then reasonable to search for quadratures that are exact for monomials of total degree lower than a given integer (and not such that the maximum degree of each individual term is lower than a given integer). Smolyak sparse quadratures, that are described in next section, have a neighboring property of polynomial exactness. They are often called “sparse grids”.

5.0 INTRODUCTION TO SMOLYAK SPARSE GRIDS

5.1 Reminder. Tensor product of quadratures

As already mentioned in section §3.6 the tensor product of 1D quadratures

$$A[f] = \sum_{i=1}^{m} a_i f(x_i) \quad \text{and} \quad B[f] = \sum_{i=1}^{n} b_i f(y_i),$$

meant to sum functions over I_1 and I_2 is

$$A \otimes B[g] = \sum_{i=1}^{m} \sum_{j=1}^{n} a_i b_j \, g(x_i, y_j),$$

tensor quadrature for functions defined over $I_1 \times I_2$. The direct extension to d-D of this tensor-product quadrature formula is

$$A_1 \otimes A_2 \otimes ... \otimes A_d[f] = \sum_{i_1=1}^{n_1} ... \sum_{i_d=1}^{n_d} w_{1i_1} ... w_{di_d} \, f(x_{1i_1}, ..., x_{di_d})$$

5.2 Hierarchy of quadratures. Difference of quadratures

All the 1D-quadratures of interest are here supposed to be part of a hierarchical set of rules, Q_l, (not necessary nested[3]). The index l is the one of the hierarchy and shall be well distinguished from the number of points of the rule (denoted n_l) and its polynomial exactness (denoted m_l). The formula of the tensor quadrature is rewritten in this case

$$Q_{l_1} \otimes ... \otimes Q_{l_d}[f] = \sum_{i_1=1}^{n_{l_1}} ... \sum_{i_d=1}^{n_{l_d}} w_{l_1 i_1} ... w_{l_d i_d} \; f(x_{l_1 i_1}, ..., x_{l_d i_d})$$

Besides, differences of quadrature formulas of the hierarchy may be defined by

$$\begin{aligned} \Delta_k[f] &:= Q_k[f] - Q_{k-1}[f] \\ Q_0[f] &:= 0. \end{aligned}$$

In general, the difference formula $\Delta_k f$ is defined on the union of the grids of the two quadratures Q_k and Q_{k-1} (which is the grid of Q_k in the nested case). Let us now note that the simple product formula with level l_1, $l_2 ... l_d$ for the successive variables may be expressed by the following sum

$$Q_{l_1} \otimes ... \otimes Q_{l_d}[f] = \sum_{\mathbf{k}/\; 1 \le k_j \le l_j} (\Delta_{k_1} \otimes ... \otimes \Delta_{k_d}) f \tag{8}$$

This property derives from the sum of the successive Δ,

$$\sum_{k=1}^{n} \Delta_k[f] = (Q_1[f] - Q_0[f]) + (Q_2[f] - Q_1[f]) + ... + (Q_n[f] - Q_{n-1}[f]) = Q_n[f],$$

and is easily checked for low dimensions. For example, the expansion of $Q_3 \otimes Q_2[f]$, is checked summing the lines then the rows (or crisscross) of the right-hand side of next equation

$$\begin{aligned} Q_3 \otimes Q_2[f] \;=\; & (Q_3 - Q_2) \otimes (Q_2 - Q_1)[f] + (Q_3 - Q_2) \otimes (Q_1 - Q_0)[f] + \\ & (Q_2 - Q_1) \otimes (Q_2 - Q_1)[f] + (Q_2 - Q_1) \otimes (Q_1 - Q_0)[f] + \\ & (Q_1 - Q_0) \otimes (Q_2 - Q_1)[f] + (Q_1 - Q_0) \otimes (Q_1 - Q_0)[f] \end{aligned}$$

5.3 Smolyak sparse grids [11]

Smolyak sparse grids are linear combinations of tensor-product operators meant to balance computational effort and accuracy. Their direct definition is based on equation (8) where the domain of indices is restricted to a simplex:

$$Q_l^d[f] = \sum_{|\mathbf{k}|_1 \le l+d-1} (\Delta_{k_1} \otimes ... \otimes \Delta_{k_d})[f] \tag{9}$$

In this expression, the weights of the tensor-product quadratures obtained when developing the Δ differences, are sums of products of weights. Besides, the lowest possible value of l is 1. The lower value of $|\mathbf{k}|_1$ for non zero terms is hence d so that the definition of sparse grids can possibly be made more explicit

$$Q_l^d[f] = \sum_{j=d}^{d+l-1} \sum_{\mathbf{k}/|\mathbf{k}|_1 = j} (\Delta_{k_1} \otimes ... \otimes \Delta_{k_d})[f] \tag{10}$$

[3] A set of quadratures (Q_l) $l \in \mathbb{N}$ is said to be nested iff all points of l-th quadrature Q_l are also quadrature points $(l+1)$-th level quadrature Q_{l+1}

The link between Q^d_{l+1} and Q^d_l (changing level) is then obviously

$$Q^d_{l+1}[f] = Q^d_l[f] + \sum_{\mathbf{k}/|\mathbf{k}|_1=d+l} (\Delta_{k_1} \otimes ... \otimes \Delta_{k_d})[f] \tag{11}$$

The link between sparse grid in dimension d and $d-1$ (changing dimension) is obtained by isolating the first index k_1 of the multi-index $\mathbf{k}$. Noting $\mathbf{k}' = (k_2, k_3 ... k_d)$, the definition (9) is rewritten

$$Q^d_l[f] = \sum_{k_1=1}^{l} \Delta_{k_1} \otimes \sum_{\mathbf{k}'/|\mathbf{k}'|_1 \leq l+d-1-k_1} (\Delta_{k_2} \otimes ... \otimes \Delta_{k_d})[f] = \sum_{k_1=1}^{l} \Delta_{k_1} \otimes Q^{d-1}_{k_1-1}$$

Of course, a direct expression in terms of the quadratures Q_l (rather than their Δ differences) is of great interest. The formula (see [4]) is

$$Q^d_l[f] = \sum_{max(l,d) \leq |\mathbf{k}|_1 \leq l+d-1} (-1)^{l+d-|\mathbf{k}|_1-1} \begin{pmatrix} d-1 \\ |\mathbf{k}|_1 - l \end{pmatrix} (Q_{k_1} \otimes ... \otimes Q_{k_d})[f] \tag{12}$$

where the lower value $|\mathbf{k}|_1$ is indeed $max(l,d)$ and not d as could be guessed from equation (9). This means that the tensor product of the lowest order quadratures are not involved in the higher order (that is higher l) formulas. They are canceled in the additive process of equation (11) when increasing the level l. The number of points $n(Q^d_l)$ involved in the sum of equation (12) depends of course of the set Q_k of 1D quadrature. An obvious upper bound may be derived from last equation

$$n(Q^d_l) \leq = \sum_{max(l,d) \leq |\mathbf{k}|_1 \leq l+d-1} n_{k_1} n_{k_2} ... n_{k_d}$$

5.4 Polynomial exactness

Tensorial product of 1D polynomials is defined as

$$\bigotimes_{i=1}^{d} \mathbb{P}^1_{m_i} = \{(x_1, ..., x_d) \in \mathbb{R}^d \rightarrow \prod_{i=1}^{d} p_i(x_i) \in \mathbb{R},\ p_i \in \mathcal{P}^1_{m_i}\}$$

where $\mathcal{P}^1_{m_i}$ is the set of mono-variable polynomials of degree lower or equal to m_i The i-th quadrature of the 1D hierarchy Q_i is assumed to have polynomial exactness m_i such that $m_i \leq m_{i+1}$ The Smolyak sparse grid quadrature

$$Q^d_l[f] = \sum_{|\mathbf{k}|_1 \leq l+d-1} (\Delta_{k_1} \otimes ... \otimes \Delta_{k_d})[f]$$

is then exact for all polynomials of the non-classical vector space

$$\mathcal{V}(Q^d_l) = Span\{\mathcal{P}^1_{m_{k_1}} \otimes ... \otimes \mathcal{P}^1_{m_{k_d}} \ / \ |\mathbf{k}|_1 = l + d - 1\}$$

Example: Assume, a series of four $(n/n+2)$ nested rules U_1, U_2, U_3, U_4 has been defined. They involve $n_1 = 1$, $n_2 = 3$, $n_3 = 5$, $n_4 = 7$ points and, as classical 1D interpolatory quadrature, their polynomial exactness are $m_1 = 0$, $m_2 = 2$, $m_3 = 4$, $m_4 = 6$. The Smolyak sparse grid U^2_4 is defined as

$$\begin{aligned} U^2_4[f] &= \sum_{j=2}^{5} \sum_{\mathbf{k}/|\mathbf{k}|_1=j} (\Delta_{k_1} \otimes \Delta_{k_2})[f] \\ U^2_4[f] &= (U_4 \otimes U_1 + U_3 \otimes U_2 + U_2 \otimes U_3 + U_1 \otimes U_4 + ...\text{lower .. order...})[f] \end{aligned}$$

From previous property, U_4^2 is exact for polynomials of non-classical vector space $\mathcal{V}(U_4^2)$

$$\begin{aligned}\mathcal{V}(U_4^2) &= Span\left\{\mathcal{P}_{m_4}\otimes\mathcal{P}_{m_1}+\mathcal{P}_{m_3}\otimes\mathcal{P}_{m_2}+\mathcal{P}_{m_2}\otimes\mathcal{P}_{m_3}+\mathcal{P}_{m_1}\otimes\mathcal{P}_{m_4}\right\}\\ \mathcal{V}(U_4^2) &= Span\left\{\mathcal{P}_6\otimes\mathcal{P}_0+\mathcal{P}_4\otimes\mathcal{P}_2+\mathcal{P}_2\otimes\mathcal{P}_4+\mathcal{P}_0\otimes\mathcal{P}_6\right\}\end{aligned}$$

$\mathcal{V}(U_4^2)$ includes all polynomials of two variables of total degree 5 and some (but not all) polynomials of total degree 6.

5.5 Number of evaluations, error analysis

These points can not be discussed independently of the selected hierarchical family of 1D quadratures Q_k. Most often, results are presented for Clenshaw-Curtis rule [2, 6]. The results derived by Novak and Ritter [8] for this choice of Q_l are presented here (but the convention of [4] is kept for indices of sparse grids).
The Q_l are the nested Clenshaw-Curtis quadratures with

$$n_1 = 1 \quad \text{then} \quad n_i = 2^{i-1}+1 \;\; (i>1) \quad \text{points.}$$

Of course, all weights of the 1D rules are positive and the degree of polynomial exactness is $m_i = n_i - 1$.
For fixed dimension d and $l \to \infty$ the number of points involved in Q_l^d, denoted $n_{(Q_l^d)}$, is equivalent (in the strong sense of limit of sequences being equal to 1) to

$$n_{(Q_l^d)} \simeq \frac{1}{(d-1)!\,2^{d-1}} 2^{l-1}(l-1)^{d-1}.$$

The largest number of points in one direction for a sparse grid based on nested quadrature is obtained for the largest of the individual k indices. The largest values of the sum of k directional quadrature indices in Q_l^d is $d+l-1$. As Q_0 is zero that largest possible single k value is l (obtained for one k_j equal l all the other equal 1). The corresponding number of points is $2^{l-1}+1$. The "tensorial counterpart" of Q^d would hence involve a full tensorial grid of $(2^{l-1}+1)^d$ points.
Besides, there exists a constant c_d depending on d only such that the L^1 norm of the vector of weights (or sum of the absolute value of these weights) of Q_l^d, denoted $SW(Q_l^d)$, is bounded by

$$SW(Q_l^d) \leq c_d (log(n_{(Q_l^d)}))^{d-1}.$$

Finally, we introduce two spaces of functions with bounded derivatives

$$C_d^r = \{f:[-1,1]^d \to \mathbb{R} \;/\; \underset{|\mathbf{k}|_1 \leq r}{\mathbf{Max}} \; ||f^{(\mathbf{k})}||_\infty < \infty\} \quad \text{and}$$

$$F_d^r = \{f:[-1,1]^d \to \mathbb{R} \;/\; \underset{|\mathbf{k}|_\infty \leq r}{\mathbf{Max}} \; ||f^{(\mathbf{k})}||_\infty < \infty\}.$$

The errors bounds of Q_l^d, $R(Q_l^q)[f]$ for functions of C_d^r and F_d^r are respectively

$$|R(Q_l^q)[f]| \leq c_{r,d}\, n_{(Q_l^d)}^{-r}\, log(n_{(Q_l^d)})^{(d-1)(r+1)}\, ||f||_\infty \quad \forall f \in F_d^r$$

and

$$|R(Q_l^q)[f]| \leq c_{r,d}\, n_{(Q_l^d)}^{-r/d}\, log(n_{(Q_l^d)})^{(d-1)(r/d+1)}\, ||f||_\infty \quad \forall f \in C_d^r$$

where of $c_{r,d}$ only depends on regularity r and dimension d and where the infinity norms refers to the max of the infinity norm of all derivatives defined respectively for functions of F_d^r and functions of C_d^r. The loss of accuracy in large dimensions due to the d factor in $n^{-r/d}$ (for C_d^r) instead of n^{-r} (for F_d^r) is sometimes also referred as the "Curse of dimensionality" (as the number of points in tensor product quadratures).

6.0 INTRODUCTION TO VARIANCE ANALYSIS

Whereas the individual influence of the inputs of a regular multivariate function f is locally estimated calculating the partial derivatives of f, Sobol' proposed a framework for a global (and hence more powerfull) analysis that attributes a part of the total variance of f on its domain of definition to each variable and subset of the variables. The associated functional decomposition is called *ANOVA representation* (*ANalysis Of VAriance*) and the corresponding fractions of variance are called *Sobol' indices* [12].

6.1 ANOVA representation

This representation is generally presented for a function f defined over $[0,1]^d$ with all inputs $(\xi_1, \xi_2, ..., \xi_d)$ following a uniform distribution over $[0,1]$. This framework is also considered here although the results are unchanged if $\boldsymbol{\xi} = (\xi_1, \xi_2, ..., \xi_d)$ follows a product law $D(\xi_1, \xi_2, ..., \xi_d) = D(\xi_1)D_2(\xi_2)...D_d(\xi_d)$.
The following representation is searched for f:

$$f(\xi) = f_0 + \sum_i f_i(\xi_i) + \sum_{i<j} f_{i,j}(\xi_i, \xi_j) + \sum_{i<j<k} f_{i,j,k}(\xi_i, \xi_j, \xi_k) + ... + f_{1,2,...,d}(\xi_1, \xi_2, ..., \xi_d) \tag{13}$$

where the integral of all the $f_{i..l}$ functions w.r.t. all their arguments shall be zero (only f_0 has not a non-zero integral over $[0,1]^d$). As a consequence of this requirement, the functions of the decomposition are orthogonal for the L_2 dot product. For example,

$$\int_{\xi_1,\xi_2...\xi_d} f_{2,3}(\xi_2, \xi_3)\ f_{1,3,4}(\xi_1, \xi_3, \xi_4)\ d\xi_1 d\xi_2 ... d\xi_d = 0$$

is proved integrating for ξ_2 or ξ_4. The demonstration of the decomposition's existence is actually constructive. Integrating over all variables, then all variables but one, then all variables but two... yields

$$\begin{aligned}
E(f) &= \int f(\xi) \prod_l d\xi_l = f_0, \\
E(f/\xi_i) &= \int f(\xi) \prod_{l\neq i} d\xi_l = f_0 + f_i(\xi_i), \\
E(f/\xi_i, \xi_j) &= \int f(\xi) \prod_{l\neq i,j} d\xi_l = f_0 + f_i(\xi_i) + f_j(\xi_j) + f_{i,j}(\xi_i, \xi_j), \\
E(f/\xi_i, \xi_j, \xi_l) &= \int f(\xi) \prod_{l\neq i,j,k} d\xi_l = f_0 + f_i(\xi_i) + f_j(\xi_j) + f_k(\xi_k) + f_{i,j}(\xi_i, \xi_j) + f_{i,k}(\xi_i, \xi_k) + f_{j,k}(\xi_j, \xi_k) + f_{i,j,k}(\xi_i, \xi_j, \xi_k)
\end{aligned}$$

and so on, which indicates how the functions of the ANOVA decomposition are successively calculated.
If f is square integrable, thanks to the orthogonality property,

$$\int f(\boldsymbol{\xi})^2 d\boldsymbol{\xi} - f_0^2 = \sum_i \int f_i(\xi_i)^2 d\boldsymbol{\xi} + \sum_{i<j} \int f_{i,j}(\xi_i, \xi_j)^2 d\boldsymbol{\xi} + \sum_{i<j<k} \int f_{i,j,k}(\xi_i, \xi_j, \xi_k)^2 d\boldsymbol{\xi} + ... + \int f_{1,2,...,d}(\xi_1, \xi_2, ..., \xi_d)^2 d\boldsymbol{\xi} \tag{14}$$

is easily deduced from equation (13). The variance of the function of interest has hence been decomposed in a sum of contributions attributable to all possible sets of variables.

6.2 Sobol' indices

The Sobol' indices are ratio of the terms of the right-hand side in equation (14) to the total variance of f,

$$Var(f) = \int f(\boldsymbol{\xi})^2 d\boldsymbol{\xi} - E(f)^2 = \int f(\boldsymbol{\xi})^2 d\xi - f_0^2.$$

They represent the part of the variance attributable to each set of variables,

$$\sigma_i = \frac{1}{Var(f)} \int f_i(\xi_i)^2 d\boldsymbol{\xi} \tag{15}$$

for individual variables,

$$\sigma_{i,j} = \frac{1}{Var(f)} \int f_{i,j}(\xi_i, \xi_j)^2 d\boldsymbol{\xi} \tag{16}$$

for pairs of variables, and so on for larger sets of variables. Of course, from equation (14),

$$\sum_i \sigma_i + \sum_{i<j} \sigma_{i,j} + \sum_{i<j<k} \sigma_{i,j,k} + ... + \sigma_{1,2,...d} = 1$$

6.3 Sensitivity indices for subsets of variables

For any subset $\boldsymbol{\xi^{sub}}$ of $\boldsymbol{\xi} = (\xi_1, \xi_2, ..., \xi_d)$, let us define by S the list of the indices of the ξ_l variables that are part of $\boldsymbol{\xi^{sub}}$. The complementary set of variables of $\boldsymbol{\xi}$ is denoted $\boldsymbol{\xi^{\overline{sub}}}$.
It is classical to define the sum of the Sobol' indices of all the subsets of $\boldsymbol{\xi^{sub}}$. This quantity is the fraction of the variance attributed by ANOVA to all combination of variables of $\boldsymbol{\xi^{sub}}$. It is also denoted here with the letter σ but with a superscript referring to the set of variables

$$\sigma^{sub} = \sum_{s=1}^{\#(S)} \sum_{(i_1<i_2<...i_s)\in S} \sigma_{i_1,i_2...i_s}$$

The so called *total index* of the variables of $\boldsymbol{\xi^{sub}}$ qualifies the fraction of the variance attributed to all sets of variables including at least one of the terms of $\boldsymbol{\xi^{sub}}$. It is denoted here $\sigma^{tot-sub}$ with a superscript referring to the set of variables. It is obviously equal to

$$\sigma^{tot-sub} = 1 - \sigma^{\overline{sub}}$$

as the terms that involve at least one variable of $\boldsymbol{\xi^{sub}}$ and those that do not involve any form a partition of all possible sets of variables.

6.4 Numerical example

The calculation of Sobol' indices is illustrated for

$$f(x, y, z) = 1 + 2x + 3x^2 + 4xy + 2y + 3z^2$$

with uniform distribution for the three variables in [0,1]. The mean and variance of f are

$$E(f) = 6 \quad Var(f) = \frac{287}{45}.$$

The first term of ANOVA decomposition is $f_0 = E(f) = 6$. The conditional expectations for one fixed variables are

$$E(f/x) = 3 + 4x + 3x^2 \qquad E(f/y) = 4 + 4y \qquad E(f/z) = 5 + 3z^2.$$

The f_1, f_2 and f_3 terms of the decomposition are then easily deduced

$$\begin{aligned} f_1(x) &= E(f/x) - f_0 = -3 + 4x + 3x^2 \\ f_2(y) &= E(f/y) - f_0 = -2 + 4y \\ f_3(z) &= E(f/z) - f_0 = -1 + 3z^2 \end{aligned}$$

The conditional expectations for two fixed variables are

$$E(f/x,y) = 2 + 2x + 3x^2 + 4xy + 2y \qquad E(f/x,z) = 2 + 4x + 3x^2 + 3z^2 \qquad E(f/y,z) = 3 + 4y + 3z^2$$

and subsequent f_{12} f_{13} and f_{23} terms of the ANOVA expansion are

$$\begin{aligned} f_{12}(x,y) &= E(f/x,y) - f_0 - f_1(x) - f_2(y) = 1 - 2x + 4xy - 2y \\ f_{13}(x,z) &= E(f/x,z) - f_0 - f_1(x) - f_3(z) = 0 \\ f_{23}(y,z) &= E(f/y,z) - f_0 - f_2(y) - f_3(z) = 0 \end{aligned}$$

that is consistent with the fact that only x and y interact in function f. Similarly

$$f_{123} = f(x,y,z) - f_0 - f_1(x) - f_2(y) - f_3(z) - f_{12}(x,y) - f_{13}(x,z) - f_{23}(y,z) = 0$$

that is, once again, consistent with the dependencies of f. The calculations can be fully or partially verified checking *a posteriori* the basis property of the decomposition,

$$E_x(f_1(x)) = 0 \quad E_y(f_1(y)) = 0 \quad E_z(f_3(z)) = 0 \quad E_x(f_{12}(x,y)) = 0 \quad E_y(f_{12}(x,y)) = 0.$$

Finally, it is checked that

$$E(f_1(x)^2) + E(f_2(y)^2) + E(f_3(z)^2) + E(f_{12}(x,y)^2) = \frac{62}{15} + \frac{4}{3} + \frac{4}{5} + \frac{1}{9} = \frac{287}{45} = Var(f)$$

The Sobol' indices are equal to

$$\sigma_x = \frac{62}{15}/\frac{287}{45} \quad \sigma_y = \frac{4}{3}/\frac{287}{45} \quad \sigma_z = \frac{4}{5}/\frac{287}{45} \quad \sigma_{xy} = \frac{1}{9}/\frac{287}{45}$$

The fraction of variance due to x y z and (x,y) jointly are respectively 64.80%, 20.90%, 12.54% and 1.74%.

6.5 Sobol's indices of a gPC expansion

Consistently with section 3.6, the results are given in 2D with the indication of how they would be extended to dD. So $\boldsymbol{\xi} = (\xi_1, \xi_2)$ and the 2D polynomial chaos is denoted

$$gF(\boldsymbol{\xi}) = \sum_{(k,l)\in\mathcal{I}} C_{k,l} P_k^{\alpha}(\xi_1) P_l^{\beta}(\xi_2),$$

where the set of exponents is most often either $\{(k,l) \mid k+l \leq M\}$ (total degree) or $\{(k,l) \mid k \leq M^1 \; ; \; l \leq M^2\}$ (individual degrees). These ANOVA formulas are given below in this second case. Let us recall that $E(gF) = C_{0,0}$ and

$$Var(gF(\boldsymbol{\xi})) = \sum_{(k,l)\in\mathcal{I} \mid 1\leq k+l} C_{k,l}^2. \tag{17}$$

The expression of variance is to be compared with equation (14) for two variables

$$Var(f) = \int f(\boldsymbol{\xi})^2 d\boldsymbol{\xi} - f_0^2 = \int f_1(\xi_1)^2 d\boldsymbol{\xi} + \int f_2(\xi_2)^2 d\boldsymbol{\xi} + \int f_{12}(\xi_1, \xi_2)^2 d\boldsymbol{\xi}.$$

The definition of the generalized polynomial chaos and the orthogonality of the basis provide an immediate identification of the f_1 f_2 and f_{12} functions of the ANOVA representation

$$\begin{aligned} f_1(\xi_1) &= \sum_{k=1}^{M^1} C_{k,0} P_k^{\alpha}(\xi_1) \\ f_2(\xi_2) &= \sum_{l=1}^{M^2} C_{0,l} P_l^{\beta}(\xi_2) \\ f_{12}(\xi_1, \xi_2) &= \sum_{(k,l)\in\mathcal{I} \mid k\geq 1\ ,\ l\geq 1} C_{k,l} P_k^{\alpha}(\xi_1) P_k^{\beta}(\xi_2) \end{aligned}$$

Obviously

$$Var(f_1) = \sum_{k=1}^{M^1} C_{k,0}^2 \qquad Var(f_2) = \sum_{l=1}^{M^2} C_{0,l} \qquad Var(f_{12}) = \sum_{(k,l)\in\mathcal{I} \mid k\geq 1\ ,\ l\geq 1} C_{k,l}^2,$$

and the sum of these three terms provides the expected decomposition of the variance (17). The three Sobol' indices σ_1, σ_2 and σ_{12} of the gPC in 2D are then calculated according to equations (15) and (16).
If d uncertain variable are involved, the variance due to interaction of variables $(\xi_{a_1}, \xi_{a_2} ..., \xi_{a_s})$ is the sum the square of the coefficients of the gPC polynomial terms involving all these variables and only these variables. The corresponding $\sigma_{a_1 a_2 ... a_s}$ Sobol' indice is obtained by dividing this sum by the total variance.

7.0 EXAMPLES OF APPLICATION

7.1 Generic missile FG5 – 3 uncertain parameters

The section summarizes a (UQ) exercise performed by DLR, USAF and ONERA in the framework of the RTO-AVT 191 group. The reference publication for this work is [9]. The considered geometry is a generic missile, called FG5, with four fins. The angle between the upper fin and the vertical plane is 22.5 degree (so that the configuration is neither what is named an "X" nor what is called a "+"). The geometry is fully defined by mathematical curves and surfaces in [9], all lengths being defined as multiples of the diameter, D, that is also used to evaluate the Reynolds number. Figure 5 presents a global view of the configuration.

Wind-tunnel measurements were carried out at two Reynolds numbers, with fixed or natural transition. During

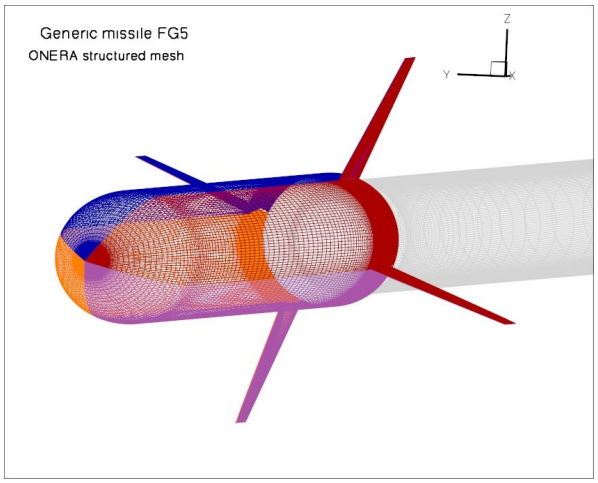

Figure 5: Wall-mesh of FG5 configuration

all the experiments, the angle of attack was varied. The experiment was repeated for verification (see figure 6 : two pink curves, short term repetition ; orange curve, tens years after repetition). Six of the experimental plots presenting forces and moments as functions of the angle of attack have been released and published in 2017 in reference [9].

The (UQ) exercise was based on the following nominal flow conditions: $M = 0.8 \quad \alpha = 12^o \quad ReD = 0.6\ 10^6$ (with fixed transition for the experiment but this option was not used in the calculations). This corresponds to the pink and orange curves of the experimental plots. The three partners first launched steady state RANS calculations using their in-house code with their favorite numerical and modelling options : ONERA ran the elsA code for (RANS) and Spalart-Allmaras model, DLR ran the TAU for (RANS) and k-w model, USAF ran the AVUS code for (RANS) and Spalart-Allmaras model. The Kp at the fin walls and the total pressure in vertical planes crossing the missile were compared in order to check main inviscid and viscous (dissipative vortices stemming from the nose) features of the flow. This comparison of nominal flows was found to be satisfactory [9].

This comparison was a good starting point for a three-parameter (UQ) exercise. Angle of attack α, upper fin angle, upper fin position were considered as stochastic variables. The three outputs of interest were the side force (CYA), the rolling moment (CLA) and the yawing moment (CNA). The reason for this choice is that they vary non-linearly in the considered interval of angle of attack. More precisely, the intervals of variation and

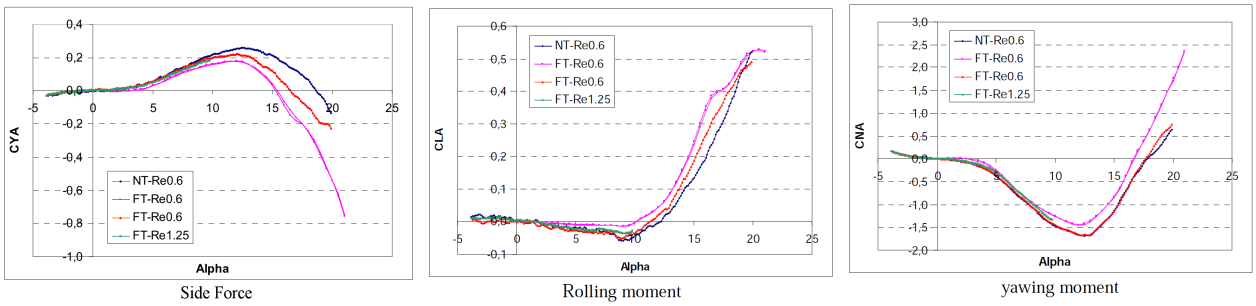

Figure 6: FG5 configuration. Measured side force, rolling moment, yawing moment as function of the angle of attack

probability density functions of the three (UQ) parameters were the following

- Angle of attack in $[10^o, 14^o]$

$$d\alpha' = (\alpha - 12)/2 \quad D^{s2}(d\alpha') = \frac{15}{16}(1 - d\alpha'^2)^2$$

- Change in upper fin azimuthal position in $[-1^o, 1^o]$

$$d\phi = \phi - 22.5 \quad D^{s3}(d\phi) = \frac{35}{32}(1 - d\phi^2)^3$$

- Upper fin angle in $[-1^o, 1^o]$

$$D^{s3}(\xi) = \frac{35}{32}(1 - \xi^2)^3$$

The joint probability of the three uncertain parameters was simply

$$D(d\alpha', d\phi, \xi) = D^{s2}(d\alpha')D^{s3}(d\phi)D^{s3}(\xi) = \frac{15}{16}\frac{35^2}{32^2}(1 - d\alpha'^2)^2(1 - d\phi^2)^3(1 - \xi^2)^3.$$

After the sign of the variation in the outputs when varying individually the three parameters have been checked, the 3-parameter (UQ) exercise was performed.

ONERA could run 31 calculations sampling the parameter space according to a Smolyak sparse grid based on (1D) Féjer second rule. Unfortunately this quadrature is not associated to the p.d.f that had to be part of the integrand... and the joint pdf of the three parameters, $D(d\alpha', d\phi, \xi)$, is a degree 16 polynomials. The sparse quadrature actually failed to correctly integrate the $D(d\alpha', d\phi, \xi)$. To solve this issue, a Kriging surrogate was fitted to the 31 evaluations of CLA and corresponding surrogates were built for CYA, CNA. Calculation of mean value and variance of the three force/moments of interest was then based on Riemann sums for (surrogate $\times$ $D(d\alpha', d\phi, \xi)$)
DLR used a surrogate-based Monte-Carlo strategy. The global calculation budget was 76 TAU simulations The simulations were run in successive series, checking intermediate results provided by the stochastic post-processing. Three Kriging surrogates were fitted to sets of 8 then 16... then 76 CLA, CYA, CNA values. At the end of the process of surrogates construction, one million Monte-Carlo samples were built from the cumulative

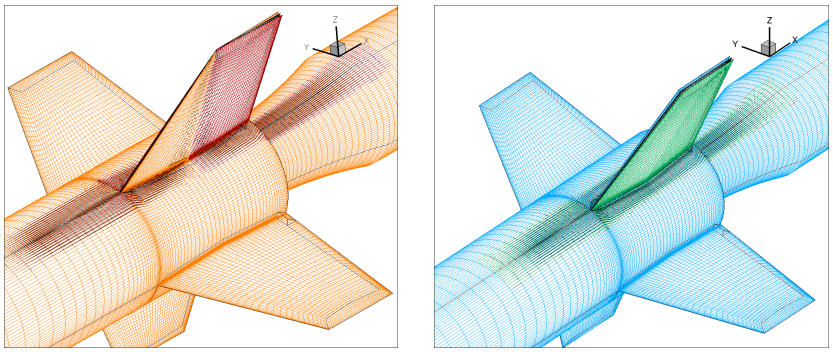

Figure 7: Visualisation of mesh deformation for fin angle (left) and fin azimuthal position (right). Both deformations need to be combined for some of the sampling points

density functions of $D^{s2}(d\alpha')$, $D^{s3}(d\phi)$ and $D^{s3}(\xi)$. Monte-Carlo mean and variance were then calculated for the Kriging surrogates based on the $D(d\alpha', d\phi, \xi)$-consistent sampling. Besides, visualisation of the p.d.f. of the outputs of interest were performed.

The calculation budget devoted to the exercise by USAF was 10 simulations. A Design of Experiment of ten points (corners of the parameters domain plus two face centers) was selected and the corresponding flows were calculated. The series of computations allowed to define a quadratic polynomial surrogate for each of the functional output of interest. Finally, a variance decomposition analysis was based on the quadratic surrogate.

The discrepancy between the results of the partners is illustrated by figure 8 that presents side-by-side, ONERA and DLR results. The difference between steady state nominal forces and moments has been considered acceptable. The difference between mean values of forces and moments has also been considered acceptable. The discrepancy between the variance of rolling moment and yawing moment was quite significant [4]. This has not been fully explained although significant differences appeared between elsA and TAU calculations in the slopes of the outputs of interest when varying only the fin angle ([9] fig. 17). This is incitement to work on both, CFD real problems and relevant mathematical functions to deepen the analysis of results, identifying the influence of the distinct CFD codes, and the influence of the distinct (UQ) methods.

Aerodynamic coefficient	Deterministic, α=12° Spalart-Allmaras	UQ, mean value Spalart-Allmaras	UQ, variance Spalart-Allmaras
CYA (side force)	0.151	0.147	1.93e-03
CLA (rolling moment)	-9.43e-03	-7.08e-03	1.09e-03
CNA (yawing moment)	-1.133	-1.105	1.03e-01

Aerodynamic coefficient	Deterministic, α=12° Wilcox k-ω, central	UQ, mean value Wilcox k-ω, central	UQ, variance Wilcox k-ω, central
CYA (side force)	0.1330	0.1291	1.3053e-03
CLA (rolling moment)	0.0446	0.0455	3.0519e-05
CNA (yawing moment)	-0.9979	-0.9708	6.1329e-02

Figure 8: Synthesis of ONERA (up) and DLR (down) results for the 3-parameter (UQ) exercise

[4] note here that it had been apparently smaller presenting standard deviation instead of variance

7.2 RAE 2822 – 3 uncertain parameters

This section summarizes a (UQ) study performed in the framework of the EU project UMRIDA (www.umrida.eu). The reference for this work is [10]. The aerodynamic configuration of interest is the well-known RAE2822 aerofoil with following flow conditions

$$\underline{M_\infty} = 0.725, \underline{\alpha} = 2.92^o, Re = 6.50 \cdot 10^6.$$

(They derive from classical corrections applied to case 6 of the experiments conducted by RAE [3].) Outputs of interest were drag, C_D, lift, C_L, and pitching moment, C_M. These coefficients were calculated with the elsA code [1] solving (RANS) equations closed by Spalart-Allmaras turbulence model. A 769$\times$ 193 mesh was used; its far-field boundary was about 1000 chord from the airfoil – see figure 9. Classical numerical options were selected and the resulting nominal discrete flow was considered as satisfactory ([10] fig. 3 and 4).

Free-stream Mach number $\underline{M_\infty}$, angle of attack $\underline{\alpha}$ and thickness to chord ratio $\underline{r} = h/c$ were then assumed to vary stochastically with the range and exponent – referring to equation (1) – displayed in Table 3. The or-

	$a = b$	X_m	X_M
ξ_1	4	$0.97 \times \underline{r}$	$1.03 \times \underline{r}$
ξ_2	4	$0.95 \times \underline{M_\infty}$	$1.05 \times \underline{M_\infty}$
ξ_3	4	$0.98 \times \underline{\alpha}$	$1.02 \times \underline{\alpha}$

Table 3: Domain of variation and exponent of β-distribution for the stochastic parameters of the RAE2822 text case

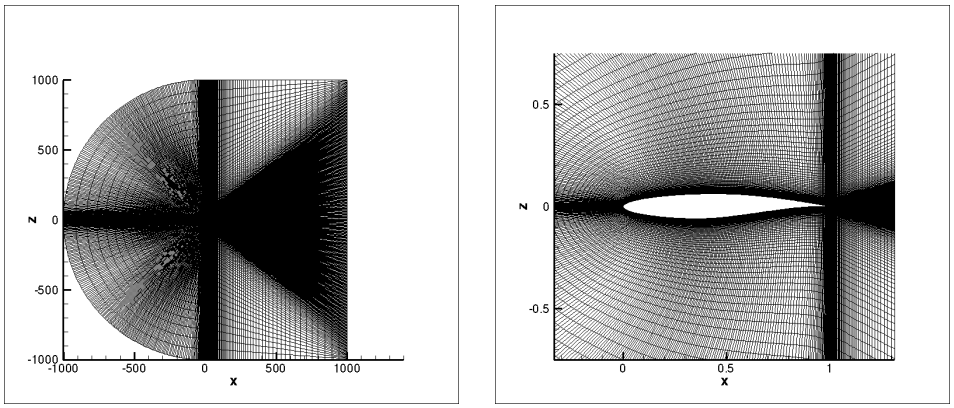

Figure 9: C structured mesh for RAE2822 calculations

thonormal polynomials associated to the common probability density function of the three uncertain parameters (after their ranges have been scaled to [-1,1]) are normalized Jacobi polynomials denoted ψ:

$$< \psi_j, \psi_k >= \int_{-1}^{+1} \psi_j(\xi)\psi_k(\xi)\, \frac{35}{32}(1-\xi^2)^3 d\xi = \delta_{jk} \quad deg(\psi_j) = j$$

It was decided to represent C_D, C_L, C_M by multivariate gPC expansions of total degree t=8. For C_D,

$$gC_D(\xi_1, \xi_2, \xi_3) = \sum_{|\mathbf{j}|_1 = j_1 + j_2 + j_3 \leq 8} c_{\mathbf{j}}\, \psi_{j_1}(\xi_1)\, \psi_{j_2}(\xi_2)\, \psi_{j_3}(\xi_3).$$

The number of coefficients $c_{\mathbf{j}}$ to calculate is the dimension of the polynomial vector space, that is, with 3 variables and total degree 8,

$$Z = \binom{t+d}{d} = \binom{8+3}{3} = \binom{11}{3} = 165.$$

The coefficients of the three gPC expansions were first calculated by quadratures, as

$$\begin{aligned} c_{\mathbf{j}} &= \int \psi_{\mathbf{j}}(\xi) C_D(\xi) D(\xi) d\xi \\ &= \int \psi_{j_1}(\xi_1)\, \psi_{j_2}(\xi_2)\, \psi_{j_3}(\xi_3) C_D(\xi_1,\xi_2,\xi_3) \frac{35^3}{32^3} (1-\xi_1^2)^3 (1-\xi_2^2)^3 (1-\xi_3^2)^3 d\xi_1 d\xi_2 d\xi_3, \end{aligned}$$

with a full-tensorial quadrature and a sparse one. Their common base is the 1D Gauss-Jacobi-Lobatto quadrature associated to the common probability density function. It is non nested (except that the extremum points are involved in the stencil of all levels). Its polynomial exactness for p points is degree $2p-3$. The tensorial quadrature was the tensor-product of the 10-point Gauss-Jacobi-Lobatto quadrature in the three directions. The sparse quadrature was the 7-th level Smolyak sparse grid based on the 1D Gauss-Jacobi-Lobatto quadrature (level p in the 1D base hierarchy corresponding to p integration points.) This sparse quadrature involves 201 points whereas, of course, the full tensorial quadrature involves $10^3 = 1000$ points. The stencils are illustrated by figure 11. The reference mean and variance were those obtained with 1000-point tensor quadrature – see table 4. It was observed that the Smolyak sparse grid based on 201 evaluations provided almost identical results.

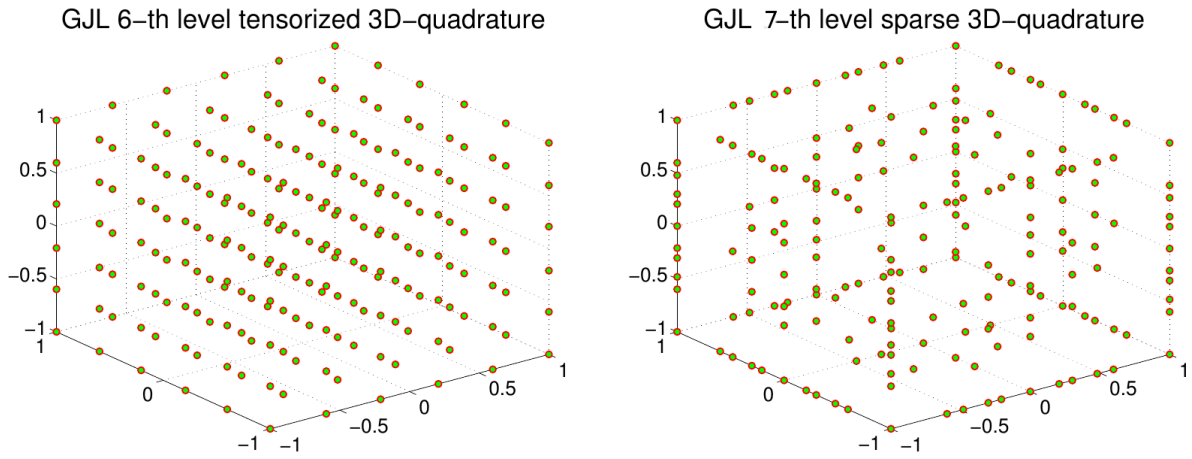

Figure 10: Visualization of 6-point tensorial Gauss-Jacobi-Lobatto quadrature and 7th level Smolyak quadrature based on Gauss-Jacobi-Lobatto quadratures – gPC coefficients are calculated with 10-point tensorial GJL and 7th level Smolyak quadrature based on GJL

Finally, a method called "compressed sensing" is used to calculate the gPC coefficients with a low number of function evaluations (that is, flow calculations), even lower than the dimension of the functional space. The collocation equations for the gPC coefficients are first recalled in explicit form,

$$\sum_{|\mathbf{j}|_1 \leq t} C_{\mathbf{j}} P_{\mathbf{j}}(\xi_k) = F(\xi_k) \quad \forall\, k \in \{1...q\}$$

	μ	σ
C_D	133.37e-04	34.128e-04
C_L	72.274e-02	1.6695e-02
C_M	-453.99e-04	32.239e-04

Table 4: RAE2822: First two moments of the aerodynamic coefficients computed by the 10–th level product rule (1000 points)

	μ	σ
C_D	133.38e-04	34.097e-04
C_L	72.269e-02	1.6729e-02
C_M	-453.96e-04	32.175e-04

Table 5: RAE2822: First two moments of the aerodynamic coefficients computed by the 7–th level sparse rule (201 points)

and in vector-matrix form ($\mathbf{F}$ column vector of F values, $\mathbf{C}$ column vector of unknown polynomial coefficients, $\mathbf{K}$ matrix $K_{ij} = P_{\mathbf{j}}(\xi_i)$)

$$\mathbf{KC} = \mathbf{F}.$$

If the number of samples is equal to the dimension of the polynomial basis ($q = Z$), a classical linear system is to be solved. If the number of samples is larger than the dimension of the polynomial basis ($q > Z$), a least square problem is to be solved. If the number of samples is smaller than the dimension of the polynomial basis ($q < Z$), compressed sensing may be used under the conditions that (1) the actual gPC expansion that is looked for, is sparse, meaning it has many coefficients very close to 0. This is often the case. This is called **"sparsity of effects"** and is verified for the searched expansions for the current test-case ; (2) a (random) sampling incoherent with the basis of polynomials is available. That is measured by the "mutual coherence"

$$\max_{\substack{1 \leq j,l \leq Z \\ j \neq l}} \frac{|K_j^T K_l|}{\|K_j\|_2 \|K_l\|_2}$$

that should exhibit the lowest possible value. The underdetermined problem

$$\mathbf{KC} = \mathbf{F}$$

is then solved by L_1 minimization

$$\mathbf{C}^* = \arg \min_{\boldsymbol{h} \in \mathbb{R}^Z} \{\|\mathbf{h}\|_1;\ \|\ \mathbf{Kh} - \mathbf{F}\|_2 \leq \epsilon\}$$

The method has been applied with as 80-point random sampling for the calculation of the 165 coefficients. The mutual coherence was found to be 0.93. The recovery of mean and variance with compressed sensing gPC was found to be satisfactory – see table 6.

	μ	σ
C_D	133.33e-04	34.052e-04
C_L	72.271e-02	1.6703e-02
C_M	-453.95e-04	32.180e-04

Table 6: RAE2822: First two moments of the aerodynamic coefficients computed by compressed sensing (80 points)

7.3 Semi-empirical helicopter flight dynamics code – analysis of variance

The comprehensive analysis code HOST is used for various helicopter studies. It has a specific capability of prediction of the aeroelastic position of rotor blades under forced motion and aeroelastic effects. An effort is in progress to study the dependency of HOST outputs w.r.t. its inputs. In a first step, the terms of the power balance of an helicopter in forward flight are considered : fuselage power P_{fus}, rotor induced power P_{ind}, profile drag power P_{prof}, total power needed by the rotor (that is the sum of the three first).
Following a basic analytical model, these terms read

$$P_{fus} = \frac{1}{2}\rho_\infty (C_x S)_f V_h^3 \qquad P_{ind} = \frac{1}{\eta_i}\frac{F_N}{2\rho_\infty S V_h}$$

$$P_{prof} = \frac{1}{8}\rho_\infty S\sigma(R\Omega)^3 Cd(1+5(\frac{V_h}{\Omega R})^2) \qquad P_{total} = P_{fus} + P_{ind} + P_{prof}$$

(where R is the rotor radius, Ω is the rotational speed, F_N is the integral of the normal forces applied to the blades, V_h is the translation speed, S is the surface of the helicopter exposed to the wind (relative to the helicopter), ρ_∞ is the far-field density, η_i is an quality factor for the rotor (=1 in the ideal case, < 1 in the real world), $(C_x S)_f$ is one single coefficient characteristic of the airframe drag that is equal to a drag coefficient multiplied by a reference surface). In this study, the three power terms result from a numerical simulation of the rotating rotor and the various coefficients (like C_x or F_N) result from integration over the blade wall and averaging over the azimuthal positions of the blade.
The case of application is the well referenced rotor 7A. All the other quantities are fixed for the model. The rotational speed (nominal 1012 rpm), Ω, and the forward translation speed (nominal 312 km/h), V_h, are considered as stochastic inputs following a normal law with a standard deviation equal to 5% of their mean value.
A Kriging intermediate model is built from a 10 points sampling after checking that this cardinal is sufficient to get a satisfactory representation of the quantities of interest. This step is involved in the (UQ) process to avoid any inconvenience due to points of the Design of Experiments that could possibly not be calculated. A gPC of total degree three is then derived for all four quantities of interest, calculating the coefficients by the dot-product formula with a (3×3) Gauss-Legendre quadrature. A Monte-Carlo sampling of the stochastic inputs and gPC evaluations lead to the sketch of the outputs p.d.f. – see figure 7.3. It is noted that profile drag power and total power exhibit non-linear responses to the Gaussian stochastic inputs.

Sobol' indices	σ_Ω	σ_{V_h}	σ_{Ω,V_h}	S_ω^{tot}	$S_{V_h}^{tot}$
fuselage power	0.64	0.36	0	0.64	0.36
rotor induced power	0	1	0	0.	1
profile drag power	0.94	0.06	0	0.94	0.06
total power	0.84	0.15	0.01	0.85	0.16

Table 7: Rotor 7A. Sobol' indices for the four power terms

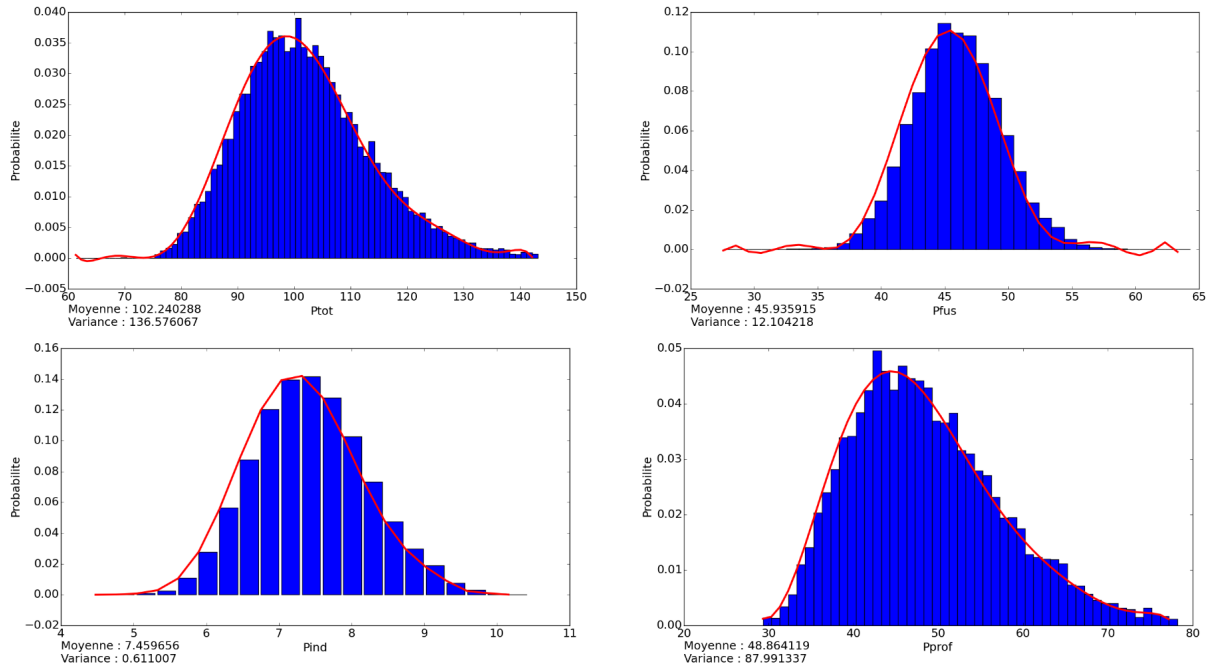

Figure 11: Visualization of power terms output p.d.f.

8.0 CONCLUSION

Definitely, Uncertainty Quantification is needed today for robust analysis and robust design using Computational Fluid Dynamics.
Unfortunately, there seems to be a lack of widely shared test problems based on inputs by aircraft industry that would be the counterpart of, for example, CRM for RANS steady-state simulation of external flows. Besides (just as for global optimisation), the efficiency of (UQ) methods can not be compared only by standard benchmarks were each partner uses its CFD code and its favorite (UQ) method(s) (see conclusions of subsection §6.1). Tests on mathematical functions (possible stemming from actual real-life test cases) are needed to isolate the specific influence of (UQ) methods.
At the end of the EU project UMRIDA (October 2016), many partners could achieve (UQ) satisfactory evaluations for 2D or 3D with 6 to 8 uncertain parameters. A great challenges consists in dealing with much larger number of uncertain parameters which will require analysis of the input space (Sobol' indices, active subspaces...) to remove inactive variables and exploitation of "sparsity of effects" whenever observed (subsection §7.2). Finally, moving towards large number of design parameters will include management of mesh deformation for possibly large number of uncertain geometrical parameters that is today a challenge.

ACKNOWLEDGMENTS

This work described in section 7.2 has been supported by the European Union's Seventh Framework Programme for research, technological development and demonstration under grant agreement #ACP3-GA-2013-605036 (UMRIDA Project www.umrida.eu).

REFERENCES

[1] Cambier, L., Heib, S., Plot., S. The $elsA$ CFD software: input from research and feedback from industry *Mechanics and Industry* Vol. 14(3) pp 159–174 (2013)

[2] Clenshaw, C.W., Curtis., A.R. A method for numerical integration on an automatic computer. *Numerische Mathematik*, (2) pp 197–205 (1960)

[3] Cook, P.H., McDonald, M.A., and Firmin, M.C.P. Aerofoil RAE 2822. Pressure distributions, and boundary layer and wake measurements. In Experimental Data Base for Computer Program Assessment. AGARD Advisory Report No. 138, NATO, May 1979; Appendix A6. (1979)

[4] Gerstner, T., Griebel, M. Numerical integration using sparse grids. *Numerical Algorithms* 18:209. (1998)

[5] Ghanem, R., Spanos, P.*Stochastic Finite Elements: a spectral approach.* Springer Verlag. (1991)

[6] Imhof, J.P. On the method for numerical integration of Clenshaw and Curtis. *Numerische Mathematik*, Vol. 5 pp 138–141 (1963)

[7] Nobile, F., Tempone, R., Webster, G. A Sparse Grid Stochastic Collocation Method for Partial Differential Equations with Random Input Data. *SIAM J. Numerical Analysis* Vol. 46(5) pp 2309-2345. (2008)

[8] Novak, E., Ritter, K. The Curse of Dimension and a Universal Method For Numerical Integration. Multivariate Approximation and Splines pp 177–187. (1997)

[9] Peter, J., Goertz, S., Graves, R. Three-parameter uncertainty quantification for generic missile FG5. AIAA Paper 2017-1197. (2017)

[10] Savin, E., Resmini, A., Peter, J. Sparse polynomial surrogates for aerodynamic computations with random inputs. AIAA Paper 433-2016 (2016)

[11] Smolyak, S.A. Quadrature and interpolation formulas for tensor products of certain classes of functions *Dokl. Akad. Nauk SSSR* pp 240–243 (1963)

[12] Sobol' I.M. Global sensitivity indices for non-linear mathematical models and their Monte-Carlo estimates. *Mathematics and Computers in Simulation* Vol. 55 pp 271–280. (2001)

[13] The homogeneous chaos. *Amer. J. Math.* Vol. 60 pp 897-936. (1938)

[14] The Wiener-Askey polynomial chaos for stochastic differential equations. *SIAM J. Numerical Analysis* Vol. 24 pp 619-644. (2002)